Efficient Multi-Robot Motion Planning for Manifold-Constrained Manipulators by Randomized Scheduling and Informed Path Generation

Weihang Guo, Zachary Kingston, Kaiyu Hang, and Lydia E. Kavraki

Abstract— **Multi-robot motion planning for high degree-of-freedom manipulators in shared, constrained, and narrow spaces is a complex problem and essential for many scenarios such as construction, surgery, and more. Traditional coupled and decoupled methods either scale poorly or lack completeness, and hybrid methods that compose paths from individual robots together require the enumeration of many paths before they can find valid composite solutions. This paper introduces Scheduling to Avoid Collisions (StAC), a hybrid approach that more effectively composes paths from individual robots by *scheduling* (adding random stops and coordination motion along each path) and generates paths that are more likely to be feasible by using bidirectional feedback between the scheduler and motion planner for informed sampling. StAC uses 10 to 100 times fewer paths from the low-level planner than state-of-the-art baselines on challenging problems in manipulator cases.**

I. INTRODUCTION

Multi-robot systems are essential for solving tasks beyond the capabilities of a single robot [1]. Multi-Robot Motion Planning (MRMP) finds continuous, collision-free paths for multiple robots, considering collisions not just with obstacles but also between moving robots. MRMP is widely used in warehouse automation and search-and-rescue; algorithms for these scenarios make simplifying assumptions (e.g., planning on a discrete grid where each robot occupies one node), enabling efficient graph search algorithms (e.g., [2]). However, while effective for many real MRMP problems, these assumptions are not applicable for arms with many degrees of freedom (DoF) in tightly constrained environments, e.g., many arms assembling together in a tight workcell, or many assistant arms in a surgery. Moreover, we consider robots with manifold-constrained end-effectors, limiting their motion to, e.g., only the planar work surface.

For high-DoF multi-robot planners, there are two essential components: *planning* individual robot paths and *scheduling* movements to avoid inter-robot collisions, similar to traffic light coordination. Standard approaches (e.g., coupled [3], decoupled [4–6], and hybrid methods [7]) make implicit or explicit trade-offs between planning and scheduling. Coupled methods plan for robots globally (e.g., dRRT [3]) and decoupled methods plan for robots individually (e.g., velocity obstacle methods [4])—both classes of methods usually

assume a fixed scheduling order, e.g., priority or simultaneous. However, these methods either fail to scale (centralized methods due to high-dimensional composite spaces) or fail to handle situations that require tight coordination (decentralized methods due to lack of global planning).

Hybrid approaches [2, 7] balance the strengths of coupled and decoupled methods by planning paths individually using a low-level planner and using a high-level planner to coordinate and schedule these paths. However, current algorithms focus on efficient enumeration of paths rather than scheduling; CBSMP [7] only checks for collisions between synchronous robot motions and considers a new set of paths if a collision is found. Thus, planning in environments such as the one shown in Fig. 1 is challenging: one arm must detour to allow the other to pass. If the arms move simultaneously, one robot must take a sufficiently long detour, which is difficult given the constrained environment. In contrast, there is a higher chance of finding a solution, and more feedback can be given to low-level planners through better scheduling.

To this end, this paper introduces the Scheduling to Avoid Collisions (StAC) algorithm, a probabilistically complete hybrid approach for MRMP in manifold-constrained, narrow, and shared workspaces for high-DoF robots. StAC's high-level planner generates many randomized schedules, which coordinate the motions to avoid collisions, for paths from a low-level planner. If the high-level planner cannot schedule a valid solution, collision information from all schedules is given to the low-level planners, who use this feedback to plan alternative paths. Our empirical results demonstrate that StAC requires 10 to 100 times fewer paths from the low-level planner to find a solution, significantly reducing planning times in highly constrained scenarios where state-of-the-art hybrid methods fail to solve even once.

II. PRELIMINARIES AND RELATED WORK

The Multi-Robot Motion Planning (MRMP) problem involves determining feasible continuous paths for a set of robots $A = \{a_1, \cdots, a_I\}$ operating in an environment W. The composite state space of all robot configurations is known as the configuration space $\mathbb{C}$, the Cartesian product of all individual robot configuration spaces $\mathbb{C}_1 \times \cdots \times \mathbb{C}_I$. Here, $\mathbb{C}_i$ represents the configuration space for robot $a_i \in A$.

We are interested in the case where each robot is *task constrained*, e.g., they must keep their end-effector on a planar work surface. We represent these constraints as *manifold constraints* and use notation from Kingston et al. [8]: the constraint imposed on robot a_i is defined as the function $f_i : \mathbb{C}_i \to \mathbb{R}^k$, which results in the implicit submanifold
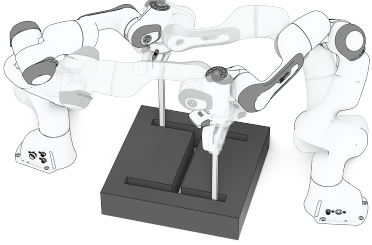
Fig. 1: We extend the classic planar doorway problem to high-DoF manipulators. The end effectors of the two arms are constrained to a manifold on the same plane. In this problem, robots must swap end-effector positions by navigating a narrow passage that only allows one robot at a time, requiring one arm to detour and wait to avoid collisions. As shown in Sec. IV-A, StAC solves the problem in an average of 5 seconds, while the state-of-the-art hybrid method fails within 60 seconds.

$\mathbb{M}_i \subset \mathbb{C}_i$ where $f_i(q) = \mathbf{0}, q \in \mathbb{M}_i$. A review of methods for planning the motion of a single manifold-constrained robot is given in [9]. The composite manifold of all constraint-satisfying configurations is given as $\mathbb{M} = \mathbb{M}_1 \times \cdots \times \mathbb{M}_I$.

The path of a_i is a continuous motion within a subset of $\mathbb{M}_i$ called the free space of a_i, denoted as $\mathbb{M}_{free,i}$. The composite constraint-satisfying free space $\mathbb{M}_{free} \subseteq \mathbb{M}$ consists of configurations in which the robots do not collide with obstacles or pairwise with each other, and satisfy constraints. Each robot a_i has an initial configuration $c_{s,i}$ and a set of goals $G_i \subset \mathbb{M}_{free,i}$. The objective is to find a continuous path with a schedule $\rho_i(s) : [0,1] \rightarrow \mathbb{M}_{free,i}$ for each robot a_i that transitions it from $c_{s,i}$ to G_i without colliding with any obstacles $o \in W$ and all other robots $a_j \in A \backslash \{a_i\}$. Initially, this path is parameterized uniformly over time, meaning $s(t) = \frac{t}{t_{final}}$ for $t \in [0, t_{final}]$, where t_{final} is the total time allocated for the robot to complete its motion from start to goal. To adjust the timing and coordination among robots, we introduce a scheduling function $\sigma_i(t) : [0, t_{final}] \rightarrow [0,1]$ that modifies the linear mapping. The actual motion of the robot is then defined as $\rho_i(t) = p_i(\sigma_i(t))$, where $\sigma_i(t)$ adjusts the progression along the path p_i.

A. Coupled Methods

Sampling-based motion planners (e.g., RRT [10], PRM [11]) can solve MRMP by treating the multi-robot system as one composite system [12]. Dedicated methods plan in factored representations, such as dRRT and variants [3, 13, 14], which efficiently sample from individual robot's configuration spaces and search in composite space. dRRT uses a prioritization rule to schedule the robots to connect two vertices in the tree. SSSP [15] iteratively builds local search spaces over individual robot roadmaps; here, all robots are scheduled to move simultaneously. McBeth et al. [16] and Choi et al. [17] used workspace topology and convex relaxation to coordinate more robots and speed up planning time. However, these cannot be directly applied to high-DoF cases due to unknown workspace-to-configuration space transformations and the complexity of the composite configuration space.

B. Decoupled Methods

Decoupled approaches address the exponential complexity of MRMP by decomposing the problem into many single-robot problems, e.g., by treating other robots as velocity obstacles and moving in simultaneously [4, 18, 19]. These methods can coordinate many planar robots but suffer in narrow workspaces, such as the doorway in Sec. IV-A, due to deadlocks. Pan et al. [20] used a potential field control policy to generate the path and a sample-based planner to escape the deadlocks. Algorithms such as [5, 21] schedule robots in prioritized order where each robot plans in order and treats previously picked robots as dynamic obstacles. Many decoupled algorithms are difficult to generalize to high-DoF cases due to unknown workspace-to-configuration space projections and differing state representations for each manipulator. Many learning-based methods [21–23] also require data and training and do not readily generalize.

C. Hybrid Methods

Hybrid methods solve MRMP by separating their approach into high-level and low-level planners. The low-level planner plans a path for one or a subset of robots, assuming they are the only robots in the environment. The high-level planner schedules and checks the feasibility of all robot paths as each robot moves along its path. If the high-level planner cannot find a valid solution, it provides feedback on conflicts between robots to the low-level planner, guiding it to generate paths that are more likely to be collision-free. The scheduling and feedback mechanisms are critical in hybrid methods. CBS [2] and LaCAM [24] are graph-based algorithms that iteratively evaluate robot paths and generate constraints for the low-level robot planner to avoid previous collisions. Modifications of CBS [25, 26] change the low-level search policy, significantly decreasing planning time and managing hundreds of robots. Due to the design of constraints in CBS, all robots move to their next state simultaneously, and no paths are scheduled. The assumption of a shared discrete representation of the robot's state space limits its ability to generate continuous motion and use it to MRMP.

CBSMP [7] adopts the CBS idea into continuous spaces, where each low-level planner maintains a roadmap instead of planning in the discrete state space. The high-level planner discretizes paths into uniform motion time segments; all agents move simultaneously. The paths are declared invalid if a collision is found, and the low-level planner replans a new path. However, many possible schedules exist to time a set of robot paths; consider cars moving on the road, where traffic lights can coordinate the cars by asking them to stop. Unlike StAC, CBSMP only explores one possible scheduling function of the paths.

D. Conflict Resolution and Path Scheduling

Given a set of robot paths, we can find how robots will follow these paths by velocity tuning [6, 12, 27, 28] which assigns each robot a velocity function and priority-based search [5] which moves each robot in priority order. Okumura [24] and Wiktor et al. [29] allow robots to stop during path

search in discrete space. Solis et al. [30] reschedules around conflict areas, using priority ordering and falling back to a composite PRM in failure cases. However, in high-DoF contexts, subproblems *still* involve planning for multiple robot arms, which remains challenging. Kasaura et al. [31] pre-compute collision pairs among vertices and edges with continuous time intervals to efficiently find collision-free intervals, but this method works only on 2D roadmaps where neighbor searches are efficient. Okumura et al. [32] used a learning-based approach to schedule paths, and such ideas can be integrated into the StAC framework to further enhance performance.

III. Scheduling to Avoid Collisions

StAC consists of the scheduler and the individual low-level motion planner $a_i \in A$ for a set of A robots. The pseudocode of StAC is given in Alg. 1. Initially, each low-level planner i plans a path $p_i(s)$ from its start to goal in its own manifold-constrained configuration space $\mathbb{M}_i$ by calling $a_i.\text{MOTIONPLAN}()$, which assumes the robot i is the only one in the environment. MOTIONPLAN() uses a projection-based manifold-constrained PRM [8] to return a path that avoids obstacles and satisfy constraints. Hence the path is specified by a set of intermediate configuration which are vertices in the roadmap. The scheduler collects all paths of the A robots into a set P. The goal of the scheduler is to find *schedules* $s_1(t), \ldots, s_A(t)$ for every path p_i in P such that there is no collision between robots or to determine that no collision-free schedule is possible and instruct the low-level planners to find a new path.

The scheduler's role is to avoid collisions between robots for the given set of fixed robot paths P (lines 8 to 15). The scheduler can avoid collisions between robots through different scheduling functions–we call this process *coordination space scheduling* (Sec. III-A). As shown in Fig. 2, SCHEDULE(P) first generates a candidate solution S^* by adding random pauses to progress to the next waypoint and assigning a random priority order to the robots to follow their paths (Sec. III-A). Collision checking is done on S^*. If S^* is collision-free with respect to all obstacles and other robots, it becomes the solution. Otherwise, the scheduler records all collision edges between robots in the *Collision Recorder* (line 14). The scheduler then iteratively reschedules for a new candidate solution using the same set of paths until reaching the maximum rescheduling attempts (N_{RA}) (Sec. III-B). After N_{RA} attempts without finding a valid solution, collision counts of all edges stored in the Collision Recorder are then batch-updated to the robots as feedback (line 18). Each robot's low-level plan1ner then stores the collision information in *Collision History*. Based on this experience, each robot plans a different set of paths P using MOTIONPLANWITHEXPERIENCE(), biased towards paths that will avoid collisions by favoring edges that have had fewer collisions with other robots in the past (Sec. III-C).

Algorithm 1 The StAC Algorithm

Input: Set of robots A, Maximum reschedule attempts N_{RA}
Output: Solution S
1: Initial motion plans $P \leftarrow \emptyset$
2: **for** each robot $a_i \in A$ **do**
3:     $p_i \leftarrow a_i.\text{MOTIONPLAN}()$
4:     $P \leftarrow P \cup \{p_i\}$
5: **end for**
6: **while** time available **do**
7:     Attempt $i \leftarrow 0$; Collision Recorder $record \leftarrow \emptyset$
8:     **while** $i \leq RA$ **do**   ▷ Iterative schedule same set of paths
9:         Candidate Solution $S^* \leftarrow \text{SCHEDULE}(P)$ ▷ Sec. III-A
10:         Collision Information $x \leftarrow \text{COLLISIONCHECK}(S^*)$
11:         **if** $x = \emptyset$ **then**
12:             **return** $S \leftarrow S^*$ ▷ Find the valid scheduling
13:         **end if**
14:         $\text{RECORDCOLLISION}(x, record); i \leftarrow i + 1$ ▷ Sec. III-B
15:     **end while**
16:     $P \leftarrow \emptyset$ ▷ Cannot find a valid scheduling. Re-plan
17:     **for** each robot $a_i \in A$ **do**
18:         $a_i.\text{UPDATE}(p_i, record[i])$ ▷ Update the feedback to robots
19:         $p_i \leftarrow a_i.\text{MOTIONPLANWITHEXPERIENCE}()$ ▷ Sec. III-C
20:         $P \leftarrow P \cup \{p_i\}$
21:     **end for**
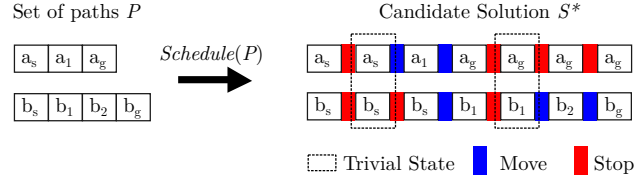22: **end while**
23: **return** $S \leftarrow \emptyset$

Fig. 2: An illustration of SCHEDULE(P). Robots a and b are in the environment with their start a_s, b_s and goal a_g, b_g. SCHEDULE(P) uses a set of individual robot paths to generate a candidate solution. The candidate solution is represented by a sequence of robot configurations. It is always in the same sequence as the path but with repetition of configurations as *stops*. To transition from composite state i to $i + 1$, each robot will either *move* or *stop*. If all robots *stop*, then state $i + 1$ is *trivial* and should be removed.

A. Scheduling in Coordination Space

In each iteration, the scheduler takes the latest set of paths P from each robot's PRM as input. Many scheduling strategies are available given P, e.g., moving simultaneously or based on a priority order, either edge-by-edge or waiting for higher-priority robots to travel from start to goal. Beyond these basic schedules, there are infinitely many possible schedules for the robots to follow their paths. The robot's path i is p_i, consisting of a sequence of configurations in $\mathbb{M}_{free,i}$. All configurations in path p_i form a set $\mathbb{P}_i \subseteq \mathbb{M}_{free,i}$. The goal of the scheduler is to find a continuous inter-robot collision-free paths schedule for all robots $\rho_i(t) : [0, t_{final}] \rightarrow \mathbb{P}_i$ for $i \in \{1 \ldots I\}$. Thus, given any time $t \in [0, t_{final}]$, $\rho_i(t)$ represents robot i's configuration $c_i \in \mathbb{P}_i$. By doing this, we constrain the range of individual scheduling functions to $\mathbb{P}_i$, which has a dimension of 1. The space of all scheduling functions for the composite system with a given set of robot paths P is called the coordination space of P.

Each robot path is a sequence of *representative configurations*, which are vertices in the PRM. We used a sampling-based method to add random stops and generate randomized scheduling functions. StAC samples stops between the
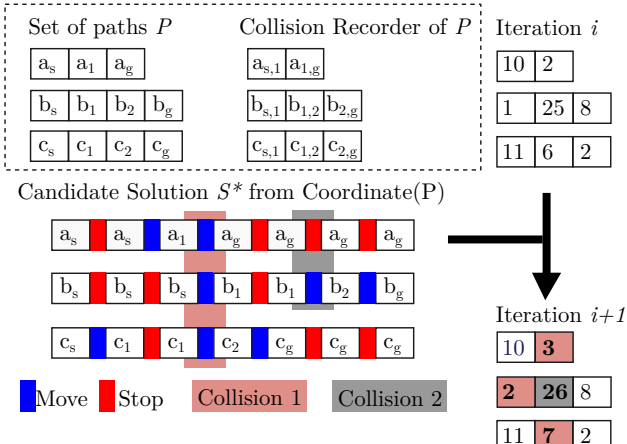
Fig. 3: The *Collision Recorder* tracks the number of collisions occurring on each edge during coordination space planning for a given set of paths, P. Each path in P initializes its Collision Record with a count of its edges, which is the path length minus one. The record for iteration i is randomly initialized for illustration purposes. During each iteration, collision checking is performed on the candidate solution, and the counter for any edge involved in a collision is incremented by one. If a robot *stops*, the collision is not counted. For example, a collision between a_g and $b_{1,2}$ in the grey region only increments the counter for $b_{1,2}$ from 25 to 26, since robot a is stopped.

Fig. 4: Low-level planners will plan a new path using the previous path in the Collision History. The number near each edge is a normalized Collision Record of the edge. The yellow region is the collision region determined by the random walk algorithm with c_1 and c_2 as its end vertices. c_d is the detour configuration. The new path is shown in the solid line.

representative configurations. We define $|p_i|$ equal to the number of representative configuration of path p_i. The total number of representative configurations across all robot paths is $L = \sum_{p_i \in P} |p_i|$. We discretize the time into L steps with all robots starting at their initial configurations at time $t_1 = 0$ and reaching their goal configurations at $t_L = t_{\text{final}}$. From t_i to t_{i+1}, the robot will either *move* from its current representative configuration to the next representative configuration or *stop* at its configuration. In the algorithm implementation, we sample $L - |p_i|$ stops for each robot to determine when it remains stationary. If all robots stop, then t_{i+1} is a trivial state and will be removed. We call the path with a scheduling function a candidate solution S^*. The length of S^*, $|S^*|$, equals to the number of non-trivial time steps. An example is shown in Fig. 2 with two robots, a and b. The paths of robot a and b have lengths of 3 and 4. Thus, 7 times steps are created. Robot a *moves* during t_2 to t_3, t_3 to t_4. Robot b *moves* during t_3 to t_4, t_5 to t_6, and t_6 to t_7, showing in blue. All robots *stop* during t_1 to t_2 and t_4 to t_5, so those two states are trivial and removed. Eventually, the length of the candidate solution equals 5.

B. Collision Recorder for Robot Feedback

After SCHEDULE(P), the original set of paths P are scheduled to form a candidate solution S^*. Despite adding stops, collisions may still occur. We use a *Collision Recorder* to log all collision edges between all robots. As shown in Fig. 3, each path in P initializes its Collision Record with a count of its edges, which is the path length minus one (i.e., the number of PRM vertices constructed the path). If no collisions are detected, a valid solution is found. Otherwise, all collisions in S^* are returned as a set of edges. In Fig. 3, two collisions are detected, showing in the red and grey regions. The Collision Recorder increments the counter for
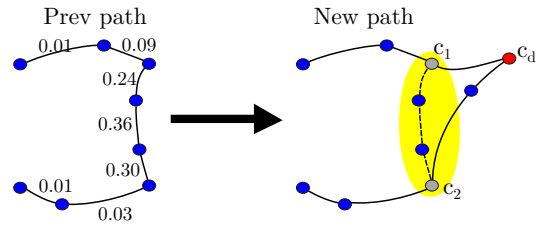
any edge involved in a collision by one. If a robot stops, the collision is not counted.

As SCHEDULE(P) iteratively samples new candidate solution of the paths, the collision recorder accumulates collision counts for different path scheduling until it finds a collision-free solution or reaches the maximum number of attempts, N_{RA}. If an edge has a higher collision count than others, it indicates that avoiding collisions on this edge is more challenging in the coordination space. Consequently, robots should avoid this region in the state space in future planning to minimize collisions.

C. Motion Planning with Experience

If no solution is found by SCHEDULE(P) after N_{RA} iterations, StAC sends the collision records to each robot's low-level planner. Each robot maintains a *Collision History* in list format. Each element in the Collision History is a pair consisting of a path and its corresponding normalized Collision Record. A normalized Collision Record divides the number of collisions on each edge by the total number of collisions, with zero collisions on edge set to 1 to avoid division by zero. The low-level planner in each robot uses the Collision History to plan different paths. The list is initialized with a "root" element containing a null path and collision record. Each time MOTIONPLANWITHEXPERIENCE() is called, the robot first selects an configuration from the Collision History based on a weighted sample. The weight of each element is assigned by a user-customized function $w(e)$. Here, we use $w(e) = a \cdot c(e) + b \cdot s(e)$, where $c(e)$ is the path cost in configuration space distance, $s(e)$ is the number of times this node has already been selected. Constants a and b adjust these contributions. Specifically, we intend to select paths with smaller costs and fewer selections. The higher $w(e)$ is, the higher the chance it is selected. $w(e)$ is always greater than 0.

If a non-root element in the Collision History is selected, a random walk algorithm is applied to select the collision region represented by the pair of vertices (c_1, c_2) shown in the yellow region in Fig. 4. The random walk algorithm randomly selects a start index in the Collision Record and performs k steps, moving either to the left or right index. The choice of moving to the left or right index is weighted by $\frac{\text{record}[idx-1]}{\text{record}[idx-1]+\text{record}[idx+1]}$. The returned vertices are the lower and upper bounds of the vertices visited. Following

the weighted sample after k iterations, the random walk algorithm increases the likelihood of selecting regions with more collisions along the path. Meanwhile, it ensures that every path interval has a non-zero chance of being selected to maintain probabilistic completeness. This path interval indicates that, regardless of how the high-level scheduler assigns the path, it often encounters a higher number of collisions with other robots. Consequently, the robot's low-level planner devises a new path around this region to avoid collisions. To plan a varied path, a detour configuration c_d is randomly sampled and required to be included in the path. The planner plans a path from c_1 to c_d and from c_d to c_2, merging them with a copy of the original path to create a new path: $(c_s, \ldots, c_1, \ldots, c_d, \ldots, c_2, \ldots, c_g)$, which is returned by MOTIONPLANWITHEXPERIENCE(). If the "root" node is selected, the robot will return MOTIONPLAN().

D. Probabilistic Completeness

The proof of probabilistic completeness for the StAC algorithm has two parts. First, we show that given a set of paths P, we eventually find a collision-free solution by calling SCHEDULE(P) with infinitely many N_{RA} if such a solution exists. Second, given infinitely many attempts for MOTIONPLANWITHEXPERIENCE(), the low-level planner (i.e., PRM with experience) of each robot will return all possible paths, including those with loops, to leverage the monotonic scheduling function.

Lemma 1. *Let P be a set of robot path. If solution S exist from scheduling robot paths P, then the length $|S| \leq \sum_{p_i \in P} |p_i|$*

Proof. Assume, for contradiction, that solution $\dot{S}$ with no trivial state exists with length $t > \sum_{p_i \in P} |p_i|$. $\dot{S}$ does not have trivial states; at least one robot must move at every transition. However, the longest simplified candidate solution $\tilde{S}$, where only one robot moves at a time, has a maximum length of $\sum_{p_i \in P}(|p_i| - 1)$. $\dot{S}$ cannot be longer than $\tilde{S}$, a contradiction. Therefore, $|S| \leq \sum_{p_i \in P}(|p_i| - 1) < \sum_{p \in P} |p|$. $\square$

Theorem 2. *Given an infinite number of reschedule attempt $N_{RA} \to \infty$, SCHEDULE(P) will eventually try every possible valid scheduling of robot paths P. Consequently, if a solution S exists in the given set P, it will be found.*

Proof. Assume, for contradiction, that there exists a valid scheduling S' of the set of robot paths P that is never constructed by SCHEDULE(P), even after an infinite number of iterations $N_{RA} \to \infty$. Let l_i be the length of the path for robot i in A and $m = \sum_{p_i \in P}(p_i)$. There are $C(l_i, m)$ possible combinations to schedule each individual path.

The probability that SCHEDULE(P) returns a specific rearrangement S' in a single iteration is $\prod_{i \in A} \frac{1}{C(l_i, m)}$. Consequently, the probability that S' is not returned in a single iteration is $1 - \prod_{i \in A} \frac{1}{C(l_i, m)}$. Thus, the probability

that S' is not returned approaches zero:

$$\lim_{N_{RA} \to \infty} P(\text{not } S') = \lim_{N_{RA} \to \infty} \left(1 - \prod_{i \in A} \frac{1}{C(l_i - 1, m)} \right)^{N_{RA}}$$
$$= 0.$$

This contradicts our initial assumption, thus SCHEDULE(P) must eventually return every possible scheduling of paths P as $N_{RA} \to \infty$. $\square$

We now show that each robot has a non-zero chance of returning all different paths (included those with loops), to compensate for the monotonicity of scheduling.

Theorem 3. *Given an infinite number of iterations $n \to \infty$ and assuming that the robot i's low-level planner is probabilistically complete, the planner will return all valid paths of robot i.*

Proof. Assume, for contradiction, that there exists a path of one robot $p = \{c_s, c_1, \ldots, c_g\}$ that is never returned by the planner, even as $n \to \infty$. Initially, the Collision History contains only the root node. The planner generates a initial path $p_{\text{temp}} = \{c_s, d_1, \ldots, d_m, c_g\}$ from c_s to c_g, which, along with its collision record, is inserted into the Collision History as element N_{temp} after scheduler schedule the path N_{RA} without finding the valid solution.

The probability of selecting N_{temp} to insert a detour path is greater than 0 using the user-customized weight function $w(e)$. Similarly, the probability of choosing (c_s, c_g) as a collision region and c_1 as a detour point is greater than 0 using the random walk algorithm and randomly sampled detour points. Therefore, the probability of planning a path $p'_{\text{temp}} = \{c_s, c_1, e_1, \ldots, c_g\}$ is greater than 0. Continuing this logic, the probability of constructing $\{c_s, c_1, c_2, f_1, \ldots, c_g\}$ by selecting (c_1, c_g) as the collision region and c_2 as the detour point is also greater than 0. This process will construct the complete path p, a contradiction. Therefore all valid paths can be generated by the robot. $\square$

Theorem 4. *Given an infinite number of iterations $t \to \infty$ and infinite maximum number reschedule attempt $N_{RA} \to \infty$, StAC will find a solution if one exists.*

Proof. According to Thm. 3, the probability that an robot returns any valid path, including those with loops, approaches 1 as $t \to \infty$. This ensures that the StAC will receive every possible combination of robot paths as $t \to \infty$.

As stated in Thm. 2, for each possible scheduling of paths, StAC will find a solution if one exists when $t \to \infty$. Therefore, given infinite iterations, the StAC is guaranteed to identify a solution if one exists. $\square$

IV. VALIDATION

We evaluate StAC's performance on teams of 7-DoF Franka Emika Panda arms constrained by a set of manifold constraints. We extend the classic 2D doorway problem to manipulators (Sec. IV-A) by constraining the end-effectors of the manipulators to a fixed orientation and to remain

Problem	Method		# of Queries			Coord.	Succ.
	Planner	N_{RA}	Q1	Median	Q3	ratio	
Case 1 (Fig. 6a)	CBSMP	-	1	1	26	11.5%	79.3%
	dRRT	-	-	-	-	-	75.7%
	StAC	1	1	1	29	20.3%	86.0%
		200	1	1	10	39.1%	**89.7%**
		400	1	1	10	37.5%	86.3%
Case 2 (Fig. 6b)	CBSMP	-	29	73	282	1.4%	42.0%
	dRRT	-	-	-	-	-	19.0%
	StAC	1	32	174	270	15.4%	47.3%
		200	3	32	99	54.2%	**64.0%**
		400	2	32	78	65.6%	61.7%

TABLE I: We randomly generated 9 start-goal pairs for each problem and tested them on the three algorithms, with each start-goal pair run 50 times and a timeout (*T/O*) of 60 seconds. For both problems, there are three subproblems where none of the planners could find a solution even once, so we excluded those subproblems for clearer visualization. We show the # of path sets the high-level planner queried from the low-level planner before finding the solution for the first quartile (Q1), median, and third quartile. *Coord. ratio* is the ratio between the total solve time and the time spent on scheduling and collision checking between robots. The CDF of solve time is shown in Fig. 7
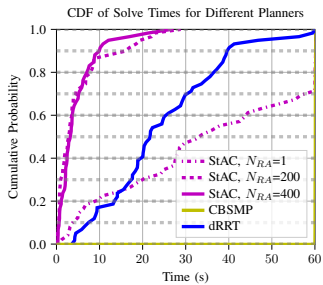

Fig. 5: CDF (Cumulative Distribution Function) of solve time for the manipulator doorway setup with two 7-DOF Franka Panda arms (shown in Fig. 1. Note that CBSMP cannot solve this problem even once, as indicated by the horizontal line at 0.

on a plane. The doorway mazes are challenging because robots must consider each other's movements and save space for others, thus requiring efficient path scheduling and cooperation between the scheduler and low-level planners. We then tested our algorithms with 3 manipulators setups (Sec. IV-B). To further test the scalability of our algorithm, we demonstrate a "cross maze" with a team of 2–5 Panda arms to navigate the narrow and shared space (Sec. IV-C). All algorithms are implemented in C++ in OMPL [33] with manifold constrained planning [8] and tested on a PC with an Intel i5-8365 1.6GHz CPU and 8GB of RAM. We utilized the MuJoCo physics engine [34] for collision detection in Scenario II and III experiments.

We used CBSMP [7] and dRRT [3] as our comparison base line. Since the source code for CBSMP and dRRT is not available, we implemented them in OMPL and added support for planning under manifold constraints. We benchmarked different map size and the number of expansions before connecting to the goal for dRRT, selecting the parameters with the best performance. Additionally, we used the same set of PRM parameters for both CBSMP and StAC.

A. 3D Doorway Setup

This setup involves a 3D doorway setup where two 7-DoF Franka Panda arms, each with an end stick, are tasked with swapping their end effector positions as shown in Fig. 1. Each algorithm was run 60 times with a timeout of 60 seconds. The arms' end effectors are constrained to move only on the xy-plane within the maze. We evaluated the performance of dRRT, CBSMP, and StAC. The solve times' cumulative distribution function (CDF) is shown in Fig. 5. StAC demonstrates superior performance compared to other state-of-the-art algorithms. CBSMP fails to solve the problem even once. This result further highlights the power of scheduling over path enumeration, as StAC only needs to sample a small detour and a stop rather than a long detour.

B. Three-manipulator Setup

(a) Case 1: Three-manipulator setup with a cross maze

(b) Case 2: Three-manipulator setup with circular arrangement
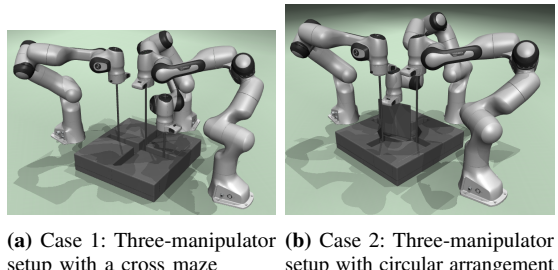
Fig. 6: Comparison of CDFs of solve times for two different three-manipulator setups: cross (Case 1) and circular (Case 2) arrangements.

Three Franka Panda manipulators perform motion planning in a clustered environment. We designed two environment setups shown in Fig. 6. In the first setup, all three manipulators have stick-shaped end effectors constrained to a plane, allowing end effector only translation at the same horizon, with one manipulator having a shorter end effector than the other two. In the second setup, two manipulators also have stick-shaped end effectors constrained to translation on the plane, while the third manipulator has a paddle-shaped end effector that can both translate and rotate within a central circular region. We randomly generated six start-goal pairs for each problem with a 60-second timeout for Case 1, and nine start-goal pairs with a 120-second timeout for Case 2, testing each pair 50 times per planner. There is one start-goal pair in Case 1 and two in Case 2 where CBSMP fails to solve even once. The result table is shown in Tab. I and Fig. 7. StAC with $N_{RA} = 200$ achieve the highest success rate for both problems.

C. Multi-manipulator Setups

To further test the scalability of StAC, We evaluate scalability on a "cross maze" scene and compare the performance of dRRT, CBSMP, and StAC. All arms' end effectors are constrained on the yz-plane, and each arm is staggered on the x-axis so that only the ends of the s-shaped end effectors will collide, as shown in Tab. II. The detail of the maze is shown Fig. 8. We randomly generated eight start-goal pairs and tested them on the three algorithms, with each
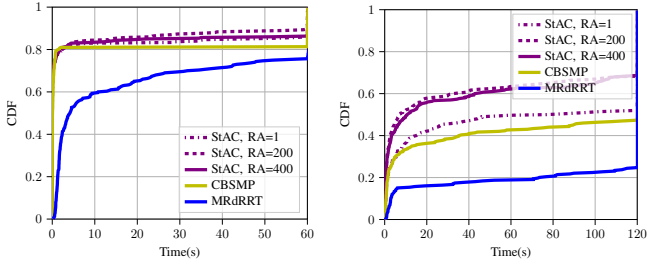
(a) Case 1 (Fig. 6a)   **(b)** Case 2 (Fig. 6b)

Fig. 7: CDFs of solve time for the 2 three-manipulator setups. In Case 1, there is one instance where CBSMP fails to solve the problem even once. Consequently, its success rate remains at 83.3%.
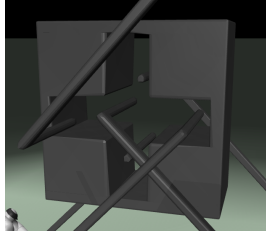

Fig. 8: The multi-manipulator setups constrain the end effector to the yz-plane within the cross area. Each arm staggered along the x-axis, so the ends of the S-shaped end effector will collide.

start-goal pair run ten times, resulting in 80 results for each algorithm. In the 2-4 arms setup, our algorithm efficiently schedules the paths within approximately ten queries in this constrained environment and shared workspace. However, as DoF increases beyond 30, the scheduler finds it more challenging to identify valid scheduling, resulting in most of the time spent on the scheduler.

D. Insight and Lessons

Our experiments show that incorporating feedback and path scheduling significantly improves multi-robot motion planning success rates and computational efficiency. By leveraging path scheduling, robots make minor detours and stops rather than large ones, which are harder to find. StAC queries fewer paths to find the solution, suggesting that our low-level planner efficiently plans collision-free paths using Collision History. The trade-off between maximum reschedule attempts (N_{RA}) and efficiency is crucial.

V. Conclusion

This paper presented the Scheduling to Avoid Collisions (StAC) algorithm for multi-robot motion planning, demonstrating its effectiveness manipulator environments with different kinds of manifold constaints. With iterative path rescheduling and an informed path generation mechanism, StAC efficiently reduces the complexity of finding collision-free solutions in shared, clustered workspaces with manifold constraints. StAC balances the search between low-level planners and the high-level scheduler. This novel high-level scheduling allows StAC to query significantly fewer paths from the low-level planner, reducing the time required to find a valid solution.

Future work will focus on developing an automated method for selecting the maximum number of rescheduling attempts. Our goal is for the algorithm to dynamically determine the optimal number of coordination attempts based on environmental conditions and robot feedback. Additionally, our algorithm is embarrassingly parallel; we will investigate the potential of leveraging parallelism to accelerate our algorithm (both CPU- and GPU-based) so that each low-level planner can plan or pre-construct multiple paths in parallel, and the high-level scheduler can schedule more than one set of paths simultaneously.

REFERENCES

[1] A. Khamis, A. Hussein, and A. Elmogy. "Multi-robot Task Allocation: A Review of the State-of-the-Art". In: *Cooperative Robots and Sensor Networks 2015*. Ed. by A. Koubâa and J. Martínez-de Dios. Cham: Springer International Publishing, 2015, pp. 31–51.

[2] G. Sharon, R. Stern, A. Felner, and N. R. Sturtevant. "Conflict-based search for optimal multi-agent pathfinding". In: *Artificial Intelligence* 219 (2015), pp. 40–66.

[3] K. Solovey, O. Salzman, and D. Halperin. "Finding a needle in an exponential haystack: Discrete RRT for exploration of implicit roadmaps in multi-robot motion planning". In: *The International Journal of Robotics Research* 35 (2013), pp. 501–513.

[4] J. Van Den Berg, J. Snape, S. J. Guy, and D. Manocha. "Reciprocal collision avoidance with acceleration-velocity obstacles". In: *2011 IEEE International Conference on Robotics and Automation*. IEEE. 2011, pp. 3475–3482.

[5] J. P. Van Den Berg and M. H. Overmars. "Prioritized motion planning for multiple robots". In: *2005 IEEE/RSJ International Conference on Intelligent Robots and Systems*. IEEE. 2005, pp. 430–435.

[6] M. Saha and P. Isto. "Multi-Robot Motion Planning by Incremental Coordination". In: *2006 IEEE/RSJ International Conference on Intelligent Robots and Systems*. 2006, pp. 5960–5963.

[7] J. I. Solis Vidana, J. Motes, R. Sandstrom, and N. Amato. "Representation-Optimal Multi-Robot Motion Planning Using Conflict-Based Search". In: *IEEE Robotics and Automation Letters* 6.3 (July 2021), pp. 4608–4615.

[8] Z. Kingston, M. Moll, and L. E. Kavraki. "Exploring Implicit Spaces for Constrained Sampling-Based Planning". In: *Intl. J. of Robotics Research* 38.10–11 (Sept. 2019), pp. 1151–1178.

[9] Z. Kingston, M. Moll, and L. E. Kavraki. "Sampling-Based Methods for Motion Planning with Constraints". In: *Annual Review of Control, Robotics, and Autonomous Systems* 1.1 (2018), pp. 159–185.

[10] J. Kuffner and S. LaValle. "RRT-connect: An efficient approach to single-query path planning". In: *Proceedings 2000 ICRA. Millennium Conference. IEEE International Conference on Robotics and Automation. Symposia Proceedings (Cat. No.00CH37065)*. Vol. 2. 2000, 995–1001 vol.2.

[11] L. Kavraki, P. Svestka, J.-C. Latombe, and M. Overmars. "Probabilistic roadmaps for path planning in high-dimensional configuration spaces". In: *IEEE Transactions on Robotics and Automation* 12.4 (1996), pp. 566–580.

[12] G. Sanchez and J.-C. Latombe. "Using a PRM planner to compare centralized and decoupled planning for multi-robot systems". In: *Proceedings 2002 IEEE International Conference on Robotics and Automation (Cat. No.02CH37292)*. Vol. 2. 2002, 2112–2119 vol.2.

[13] R. Shome, K. Solovey, A. Dobson, D. Halperin, and K. E. Bekris. "dRRT*: Scalable and informed asymptotically-optimal multi-robot motion planning". In: *Autonomous Robots* 44.3 (Mar. 1, 2020), pp. 443–467.

[14] A. Solano, A. Sieverling, R. Gieselmann, and A. Orthey. *Fast-dRRT*: Efficient Multi-Robot Motion Planning for Automated Industrial Manufacturing*. Sept. 19, 2023.

[15] K. Okumura and X. Défago. "Quick Multi-Robot Motion Planning by Combining Sampling and Search". In: *Proceedings of the Thirty-Second International Joint Conference on Artificial Intelligence, IJCAI-23*. Aug. 2023, pp. 252–261.

[16] C. McBeth, J. Motes, D. Uwacu, M. Morales, and N. M. Amato. "Scalable Multi-Robot Motion Planning for Congested Environments With Topological Guidance". In: *IEEE Robotics and Automation Letters* 8.11 (2023), pp. 6867–6874.

Problem	Method		Planning Statistics						Coord.	Succ.
			Q1		Median		Q3%		ratio	
	Planner	N_{RA}	T	Q	T	Q	T	Q		
	dRRT	-	0.016	-	0.042	-	0.068	-	-	**100.0%**
	CBSMP	-	0.015	1	0.099	14	0.160	11	10.3%	**100.0%**
	StAC	1	0.015	1	0.021	1	0.029	1	38.6%	**100.0%**
		200	**0.013**	1	**0.017**	1	0.023	1	36.5%	**100.0%**
		400	0.014	1	**0.017**	1	**0.022**	1	34.0%	**100.0%**
		400	0.015	1	0.018	1	0.028	1	4.3%	**100.0%**
	dRRT	-	1.398	-	2.794	-	5.242	-	-	**100.0%**
	CBSMP	-	0.996	31	2.906	145	8.162	315	3.1%	94.4%
	StAC	1	0.086	1	0.737	8	2.459	22	35.1%	**100.0%**
		200	**0.057**	1	**0.085**	1	**0.177**	1	**84.7%**	**100.0%**
		400	0.061	1	0.092	1	0.192	1	87.2%	**100.0%**
		400	0.058	1	0.098	1	0.249	1	91.3%	**100.0%**
	dRRT	-	7.926	-	37.143	-	T/O	-	67.1%	
	CBSMP	-	0.524	31	13.009	516	T/O	2041	5.5%	68.9%
	StAC	1	0.561	6	5.078	60	T/O	412	58.6%	72.2%
		200	**0.075**	1	0.621	2	28.174	26	92.7%	82.2%
		400	0.098	1	1.326	3	**23.586**	20	97.6%	**84.4%**
		400	0.083	1	**0.313**	1	T/O	17	94.6%	73.3%
	dRRT	-	T/O	-	T/O	-	T/O	-	-	-
	CBSMP	-	6.960	274	23.347	745	T/O	1813	4.4%	65.6%
	StAC	1	54.344	308	T/O	349	T/O	385	53.4%	25.6%
		200	26.911	11	T/O	22	T/O	28	97.7%	30.0%
		400	28.761	11	T/O	16	T/O	19	96.0%	33.3%
		400	T/O	11	T/O	14	T/O	15	97.3%	20.0%

TABLE II: We randomly generated 8 start-goal pairs for each problem and tested them on the three algorithms, with each start-goal pair run 10 times and a timeout (*T/O*) of 60 seconds, resulting in 80 results for each algorithm. We show the results for the first quartile (Q1), median, and third quartile (Q3%). The *T* refers to the total solve time. *Q* is the number of path sets the high-level planner queried from the low-level planner before finding the solution. *Coord. ratio* is the ratio between the total solve time and the time spent on scheduling and collision checking between robots.

[17] C. Choi, M. Adil, A. Rahmani, and R. Madani. "Multi-Robot Motion Planning via Parabolic Relaxation". In: *IEEE Robotics and Automation Letters* 7.3 (2022), pp. 6423–6430.

[18] K. Guo, D. Wang, T. Fan, and J. Pan. "VR-ORCA: Variable Responsibility Optimal Reciprocal Collision Avoidance". In: *IEEE Robotics and Automation Letters* 6.3 (2021), pp. 4520–4527.

[19] S. H. Arul and D. Manocha. "V-RVO: Decentralized Multi-Agent Collision Avoidance using Voronoi Diagrams and Reciprocal Velocity Obstacles". In: *2021 IEEE/RSJ International Conference on Intelligent Robots and Systems (IROS)*. 2021, pp. 8097–8104.

[20] T. Pan, C. K. Verginis, A. M. Wells, L. E. Kavraki, and D. V. Dimarogonas. "Augmenting Control Policies with Motion Planning for Robust and Safe Multi-robot Navigation". In: *2020 IEEE/RSJ International Conference on Intelligent Robots and Systems (IROS)*. 2020, pp. 6975–6981.

[21] W. Li, H. Chen, B. Jin, W. Tan, H. Zha, and X. Wang. "Multi-Agent Path Finding with Prioritized Communication Learning". In: *2022 International Conference on Robotics and Automation (ICRA)*. 2022, pp. 10695–10701.

[22] Q. Li, W. Lin, Z. Liu, and A. Prorok. "Message-Aware Graph Attention Networks for Large-Scale Multi-Robot Path Planning". In: *IEEE Robotics and Automation Letters* 6.3 (2021), pp. 5533–5540.

[23] J. Foerster, N. Nardelli, G. Farquhar, T. Afouras, P. H. Torr, P. Kohli, and S. Whiteson. "Stabilising experience replay for deep multi-agent reinforcement learning". In: *International conference on machine learning*. PMLR. 2017, pp. 1146–1155.

[24] K. Okumura. "LaCAM: Search-Based Algorithm for Quick Multi-Agent Pathfinding". In: *Proceedings of the AAAI Conference on Artificial Intelligence* 37.10 (June 2023), pp. 11655–11662.

[25] M. Barer, G. Sharon, R. Stern, and A. Felner. "Suboptimal variants of the conflict-based search algorithm for the multi-agent pathfinding problem". In: *Proceedings of the international symposium on combinatorial Search*. Vol. 5. 1. 2014, pp. 19–27.

[26] J. Lim and P. Tsiotras. "CBS-Budget (CBSB): A Complete and Bounded Suboptimal Search for Multi-Agent Path Finding". In: *arXiv preprint arXiv:2206.00130* (2022).

[27] K. Kant and S. W. Zucker. "Toward Efficient Trajectory Planning: The Path-Velocity Decomposition". In: *The International Journal of Robotics Research* 5 (1986), pp. 72–89.

[28] T. Simeon, S. Leroy, and J.-P. Lauumond. "Path coordination for multiple mobile robots: a resolution-complete algorithm". In: *IEEE Transactions on Robotics and Automation* 18.1 (2002), pp. 42–49.

[29] A. Wiktor, D. Scobee, S. Messenger, and C. Clark. "Decentralized and complete multi-robot motion planning in confined spaces". In: *2014 IEEE/RSJ International Conference on Intelligent Robots and Systems*. 2014, pp. 1168–1175.

[30] I. Solis, J. Motes, M. Qin, M. Morales, and N. M. Amato. "Adaptive Robot Coordination: A Subproblem-based Approach for Hybrid Multi-Robot Motion Planning". In: *IEEE Robotics and Automation Letters* (2024), pp. 1–8.

[31] K. Kasaura, M. Nishimura, and R. Yonetani. "Prioritized Safe Interval Path Planning for Multi-Agent Pathfinding With Continuous Time on 2D Roadmaps". In: *IEEE Robotics and Automation Letters* 7.4 (2022), pp. 10494–10501.

[32] K. Okumura, R. Yonetani, M. Nishimura, and A. Kanezaki. "CTRMs: Learning to Construct Cooperative Timed Roadmaps for Multi-Agent Path Planning in Continuous Spaces". In: *Proceedings of the 21st International Conference on Autonomous Agents and Multiagent Systems*. AAMAS '22. International Foundation for Autonomous Agents and Multiagent Systems, 2022, pp. 972–981.

[33] I. A. Şucan, M. Moll, and L. E. Kavraki. "The Open Motion Planning Library". In: *IEEE Robotics & Automation Magazine* 19.4 (Dec. 2012). https://ompl.kavrakilab.org, pp. 72–82.

[34] E. Todorov, T. Erez, and Y. Tassa. "MuJoCo: A physics engine for model-based control". In: *2012 IEEE/RSJ International Conference on Intelligent Robots and Systems*. 2012, pp. 5026–5033.